Lasers in Surgery and Medicine 18:121–128 (1996)

# Dentin Ablation With Three Infrared Lasers

**Joseph Neev, PhD, Kevin Pham, BS, Jon P. Lee, and Joel M. White, DDS**

*Beckman Laser Institute and Medical Clinic, Irvine 92715 (J.N., K.P., J.P.L.); University of California, San Francisco (J.M.W.), California*

***Background and Objective*: Lasers are used for caries removal in enamel and dentin, but are currently limited in their ability to remove sound tooth structure. In this study plasma interaction regimes are investigated as the principal factor determining the ablation characteristics.**

***Study Design/Materials and Methods*: Three ablation parameters are considered: ablation rates (AR), surface temperatures (ST), and surface morphological characteristics. The three lasers investigated were Er:YSGG with wavelength (WL) of 2.94 μm and pulse duration (PD) of 250 μs, Ho:YSGG at 2.1 μm and 250 μs and an Nd:YAG with WL of 1.06 μm and PD of 15ns.**

***Results*: The highest surface temperatures were observed during Er:YSGG treatment (> 300°C), moderate temperatures with the Ho:YSGG (150°C), and lowest with the Nd:YAG (with highest surface temperature generally lower than 80°C). Ablation rates were also compared and were shown to be highest with the Er:YSGG and Ho:YSGG, and lower with the Nd:YAG (< 3 μm). In all systems, efficient ablation was observed only in the presence of plasma. In spite of their different wavelengths, for similar spot sizes, energy, and pulse duration, ablation rates of Ho:YSGG and Er:YSGG were found to be comparable. These were an order of magnitude larger than the ablation rates observed with the nanosecond system.**

***Conclusion*: Possible explanation for these observations is given in terms of plasma characteristics.** © 1996 Wiley-Liss, Inc.

**Key words: plasma, laser-tissue interaction, thermal, mechanical**

## INTRODUCTION

Lasers were introduced to dental research in the early 1960s and are now used in several specific areas of application. These include surgical laser treatment of oral malignancies and periodontal diseases, dental caries detection and control, and preparation and sterilization of root canals [1]. In spite of these advances, lasers are still limited in their ability to remove sound tooth structure since elevating the temperature in the tooth can generate adverse effects at the surface and in the tooth pulp. Ablation efficiency, thermal damage, and final surface characteristics are, of course, the ultimate tests to any laser effectiveness.

In the past few years, several infrared (IR) lasers have been advocated for hard tissue applications [2–14]. In particular, Er:YAG in a normal spiking mode (PD of ~ 200 μs), has been proposed as a leading candidate for efficient hard tissue ablation since its high absorption coefficient allows for a large energy/volume deposition and minimal heat diffusion, which improves ablation rates with minimal collateral thermal damage.

In this study we compare three different IR laser systems: two (Er:YSGG and Ho:YSGG) of similar pulse duration and one (Q-switched Nd:YAG) of considerably shorter pulse duration. For a given parameter set, the ablation characteristics of the two long pulse lasers are surprisingly

Accepted for publication December 28, 1994.

Address reprint requests to Dr. Joseph Neev, Beckman Laser Institute and Medical Clinic, Irvine, CA 92715.

similar, whereas the ablation rates and surface characteristics of the Q-switched laser are remarkably different. The ablation characteristics of the Q-switched Nd:YAG, in contrast, are very similar to those of other nanosecond systems [15,16], even though their wavelength-dependent absorption characteristics are remarkably different. Similarly, ablation characteristics of the normal spiking mode Ho:YSGG and Er:YSGG lasers are quite comparable to those of the Nd:YAG in its normal pulse mode operation [17]. Our observations are then explained in terms of the regime of plasma generation, which, we believe, is the dominant mechanism governing these ablation effects.

## MATERIAL AND METHODS

Ablation studies were performed using thin dentin slices. Dentin slices, 0.5–1.0 mm thick, were cut from the middle section of freshly extracted third molars in a plane perpendicular to the occlusal-cervical direction. Teeth were treated with 0.5 M EDTA for 2 minutes to remove the smear layer, then stored in 10% thymol solution until treatment. Enamel was sliced parallel to the crown and washed with demineralized water.

**Laser parameters.** Three laser systems were used: Er:YSGG and Ho:YSGG with pulse duration (PD) of 250 μs (normal pulse mode) and wavelengths (WL) of 2.79 and 2.08 μm, respectively, and a Q-switched Nd:YAG with PD of 15 ns and WL of 1,064 μm. Wherever possible, the following parameters were used in each laser system: energy per pulse = 25, 50, and 75 mJ, fluence = 2, 4, 6, and 8 J/cm$^2$ pulse repetition rate (PRR) = 1,5,9 Hz.

**Ablation rates.** These rates were determined by aiming a He-Ne probe beam collinearly with the ablating laser. Detection of the He-Ne beam designated slice penetration, thus providing a well defined endpoint for the measurements. From the measurement of time elapsed from ablation start to He-Ne penetration, combined with the laser known pulse repetition rates, the exact number of pulses and ablation removal rates were calculated.

**IR thermography.** A thermal camera (Inframetrics Model 600 Imaging Radiometer, Bedford, MA) with a scan speed of 32 frames per second was used for temperature measurements. The center temperature adjustment ranges from 20°C to 1,500°C. The camera field of view could be adjusted from 1:1 to 8:1, and was maintained at 2:1 or 4:1. The camera detector was a liquid-nitrogen-cooled HgCdTe with spectral sensitivity from 8–12 μm. The thermal camera was placed so that the surface temperature (ST) could be viewed directly. The camera was operated in the "point mode" so that center temperature could be read with the camera specified accuracy of ±0.5°. Post-ablative surface characteristics (degree of charring, cracking, or other surface deformation) were evaluated using light microscopy (SZH-ILLD Olympus Optical CO, Japan) at a magnification of 60×.

The ablation rates for the 15 nanosecond Q-switched Nd:YAG laser are shown in Figure 1a. This system is characterized by the lowest ablation rates. AR range from ~ 1 μm/pulse at 20 mJ/p energy, to ~ 2.5 μm/pulse at 80 mJ. No significant dependence on pulse repetition rate (PRR) was found.

Ablation rates with the Ho:YSGG system are illustrated in Figure 1b. AR are almost an order of magnitude improved compared to that of the nanosecond Nd:YAG system. Maximum ablation rates observed at 75 mJ/p are between 17 and 18 μm/pulse. Ablation rates are considerably lower at 50 mJ/pulse and lowest at 25 mJ/Pulse where they range from 6–8 μm/pulse. No clear trend in the dependence of AR on pulse repetition rates could be identified.

AR for the Er:YSGG system are shown in Figure 1c. Interestingly, Er:YSGG laser AR over the range of energies tested for the other two systems is not much higher than that of the Ho:YSGG. Since AR at the *lower* energy levels are more than twice as efficient at 1 Hz as those at 5 Hz, PRR appears to play a role in this energy regime. Note that this trend disappears at higher energies (> 140 mJ/p). At *higher energies* (> 100 mJ/p), AR at 1 Hz remain relatively constant with respect to increasing pulse energy, whereas AR at 9 Hz increase linearly from 24–47 μm/pulse, and AR at 5 Hz increase from 20 μm/pulse to > 90 μm/p.

In both Er:YSGG and Ho:YSGG systems, AR were poor unless a laser-induced plasma was formed. In the short pulse Nd:YAG, ablation plasma was always present.

### IR Thermography

Figure 2a shows ablation hotspot (HS) temperatures for the nanosecond Nd:YAG system.

There appears to be a linear dependence of HS temperature on PRR. The temperature dependence on energy (or fluence) does not appear significant at 1 and 5 Hz, but does increase linearly at 10 Hz. HS temperatures of this system are by far the lowest of all three IR systems and are comparable to the ablation temperatures obtained with nanosecond excimer lasers. Note also that at PRR of 1 Hz, HS temperature, although remaining very close to ambient (within the time resolution of the relatively slow camera scan), does appear to increase slightly at 40 mJ/p and 80 mJ/p.

Figure 2b shows the ablation temperatures of the Ho:YSGG system. Clearly, temperatures are considerably higher compared to the nanosecond Nd:YAG. Unlike the Nd:YAG system, HS temperatures at 1 Hz increase significantly with energy and range from > 40°C at 20 mJ/pulse to ~ 90°C at 80 mJ/pulse. At 5 Hz, the increase in temperature is from 65°C at 20 mJ/p to ~ 140°C at 80 mJ/p. At 9 Hz, HS temperatures increased from ~ 90°C at 20 mJ/p to 120°C at 60 mJ/p. Due to the laser output limitations at the higher PRR of 9 Hz, HS temperatures were not obtained at 80 mJ/pulse. At 9 Hz, HS temperatures increased significantly with energy but remained within the experimental uncertainty when compared to the corresponding energies at 5 Hz.

Ablation HS temperatures for the Er:YSGG system ranged from 40°C at 1 Hz and 20 mJ to >180°C for the same energy at 9 Hz. Temperatures >230°C were measured at 80 mJ per pulse at 5 Hz. Again, even at 1 Hz an increase over the ambient room temperature is observed. A dependence on pulse energy at this low PRR is observed only as the energy is increased from 20–50 mJ/p. At 5 Hz, the temperature increases very rapidly from 50°C to ~ 190°C as energy is raised from 20–50 mJ/p. Temperatures then increase further to 230°C at 80 mJ/p. It is interesting that at 5 Hz and 20 mJ/P, HS temperature remains very close to the 1 Hz level (50°C). Thermal effects at 9 Hz were tested only at 20 mJ/p where HS temperatures of 180°C were measured.

### Surface Characteristics

Light microscopy observations of the ablated surface were performed to determine surface conditions. Following is a summary of each laser system's effects.

**Nd:YAG.** At *1 Hz,* no charring was observed at all pulse energies tested (40 and 80 mJ/p). Microscopic examination showed a surface glazed in appearance that looked similar to that of the XeCl excimer lasers [16]. A more detailed examination for similarities will be possible with scanning electron microscopic studies. For *5 Hz,* no chars or cracks were observed at both 40 and 80 mJ. Again, the clean appearance of the surface resembled that of the XeCl excimer. For *10 Hz,* a very clean ablation surface was produced at 40 mJ/P with no evidence of charring. Occasional cracks appeared in a concentric configuration (~ 2–3 cracks per crater). At 80 mJ/P, 3–4 cracks per hole were observed, along with the glazed appearance of the surface. Still no charring was detected.

**Ho:YSGG.** At the lowest energy, very little charring was observed. Some melted granules were already apparent. These granules were 40–80 μm in diameter and half-sphere in shape. Ablation at 1 Hz and 5 Hz showed even less charring than at 9 Hz. At twice the energy, the amount of charring was increased, but no cracks were observed. Molten granules were present. This general characteristic persisted despite changing the PRR (1, 5, and 9 Hz). Further increases in pulse energy to 75 mJ resulted in some cracks and a small increase in the amount of charring. Further increases in PRR resulted in increased charring and cracking.

**Er:YSGG.** At *1 Hz* and 40 mJ/p per pulse, no cracking and very little charring was observed; on the other hand, no melting could be detected (which appears to indicate mechanical tearing). At 60 mJ/p and 80 mJ/p, still no charring or any other visible signs of thermal damage were observed. Only at 160 mJ/p per pulse do we begin to see very minimal charring along the wall. Even at 200 mJ/p, very little charring was observed at this low PRR. At *5 Hz,* heating effects became quite severe with close to 50% of the surface charred, even at 60 mJ/p, the lowest energy level tested. Some melted granules began to form as in the Ho:YSGG case, yet no cracking was observed. At 80 mJ/p, more than 50% of the surface was charred, some melted granules (40–80 μm) were formed (similar to the Ho:YSGG), but still no cracking was observed. At 200 mJ/p, more melting and charring were observed, along with some cracking. Depth of thermal damage penetration was observed to be ~ 5–10 μm. At *9 Hz,* the heat generated by this high PRR created considerable charring and some cracking even at a comparatively low pulse energy of 80 mJ/p. At a pulse energy of 160 mJ/p, similar effects were noted.

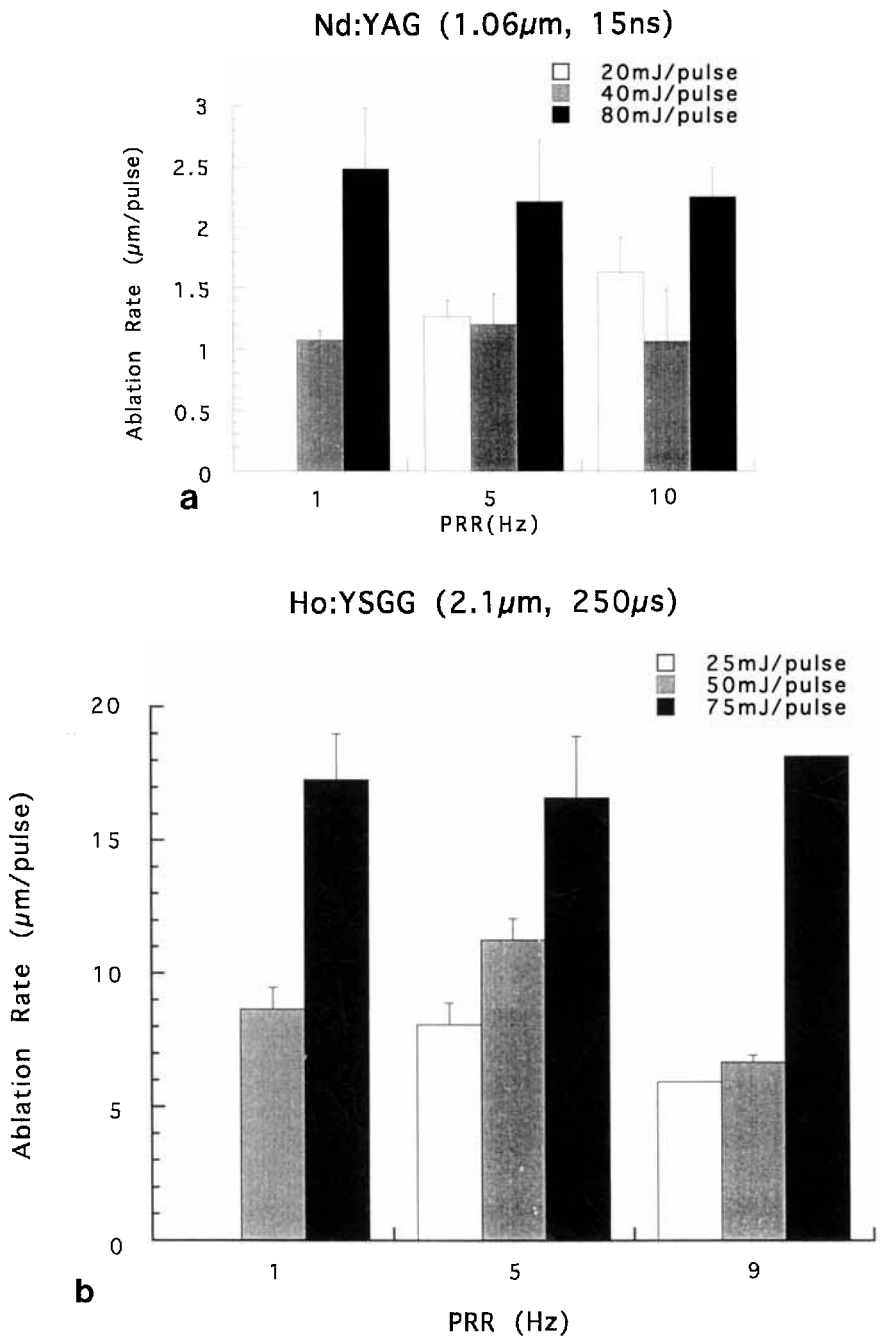


Fig. 1. Ablation rates: (a) for the Q-switched Nd:YAG laser, (b) with the Ho:YSGG laser, (c) for the Er:YSGG laser.

## DISCUSSION

When the results presented above are considered in the context of established experience with other nanosecond and normal pulse systems, we find several parallel features that are influenced more by pulse duration then by WL-dependent absorption characteristics. "Signature" AR and surface temperatures of the 15 nanosecond Q-switched Nd:YAG in our experiments are quite similar to those observed for a 15ns XeCl excimer laser [20]. In fact, AR of these two systems for 5 Hz and 10 Hz fall approximately on the same curve. AR for the ArF Excimer are of the same order of magnitude as well [20], and surface temperature characteristics are very similar. In all such systems, surface temperatures are confined

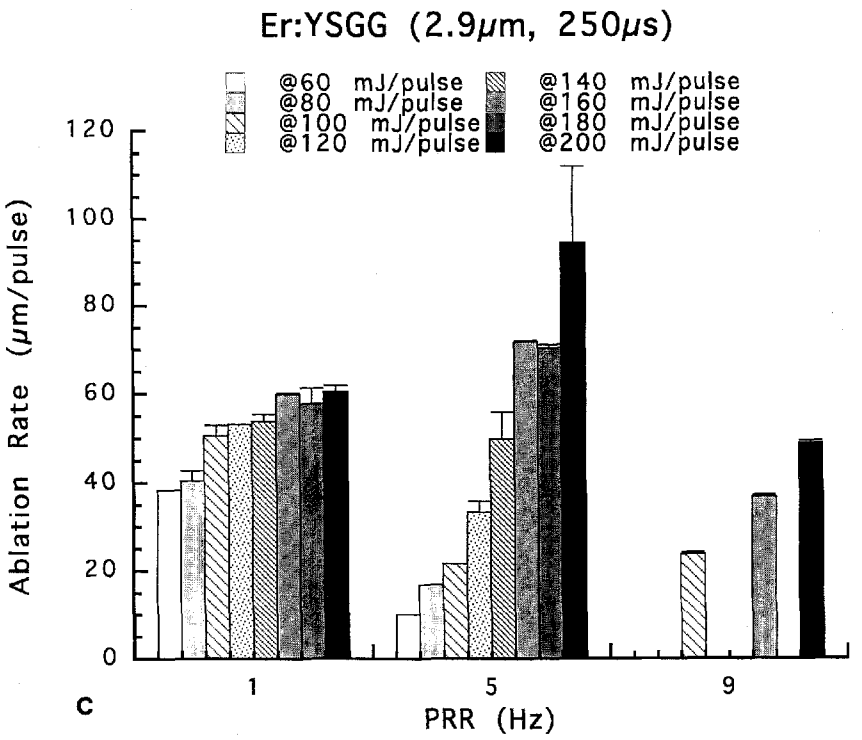


Fig. 1c

to < 100°C even at the highest PRR and energy levels tested (in our ns Nd:YAG—10 Hz and 80 mJ/p).

Similarly, AR of the longer normal mode pulse systems such as the Er:YSGG, Ho:YSGG, and Nd:YAG [17] are also quite similar to each other. Again, these similarities are not expected if the great variation in WL absorption characteristics is considered. It is interesting to note that our own observations in this regard resemble those of another group that compared AR of a TEA $CO_2$ laser and a normal pulse Er:YAG [23]. Whereas the PD of these two systems was significantly different (2 μs and 250μs, respectively), the fact that ablation rates of guinea pig skin fell on the same fluence-etch depth curve in these two very different systems is intriguing. From such observations it appears that, in the higher peak power regimes discussed here, WL-absorption characteristics do not affect AR as strongly as is usually suggested.

An alternative parameter that is often assigned a great deal of significance is the laser PD. If we consider pulse duration and temporal structures, we can categorize the laser interaction according to the difference between the two pulse regimes. The interaction mechanism is indeed often explained in terms of thermal and stress confinement characteristics [22], which are defined as the ratio of the tissue stress and thermal relaxation times to the laser PD. In the above Ho:YSGG and Er:YSGG experiments, however, we observed that AR with a predetermined pulse duration and pulse energy changed dramatically once laser-induced plasma—a hot gas of electron and ions—was formed.

Although PD and WL-dependent absorption certainly do play a role in determining ablation characteristics, based on the above observations, we propose that this role should be considered in terms of plasma generation and plasma-mediated coupling of laser energy. In particular, it appears that for normal mode systems an efficient ablation at a given parameter set (PD, pulse energy, spot size, etc.) does not proceed until plasma is initiated. Once plasma is initiated, an efficient coupling of energy is possible and ablation proceeds.

Ablation of hard tissue follows the deposition of laser energy in matter. Energy deposition is achieved through direct tissue absorption (linear or nonlinear) or through laser-driven plasma coupling. In plasma-free ablation (PFA), material can be removed by such processes as vaporization, melt removal, and pyrolysis or burning. It is also suggested that mass removal can be generated

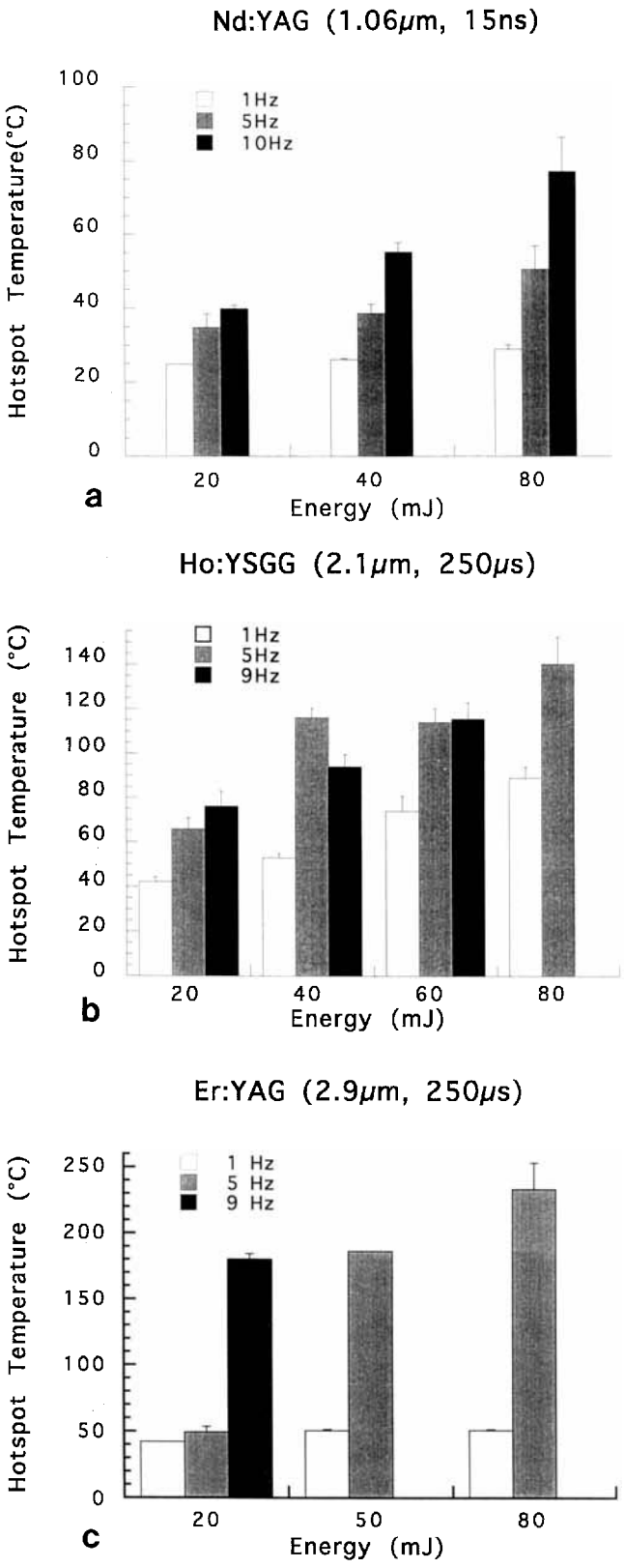


Fig. 2. Ablation hotspot temperatures: (**a**) for the Q-switched Nd:YAG laser, (**b**) for the Ho:YSGG laser; (**c**) for the Er:YSGG laser.

through material fragmentation by bond-breaking high-energy UV photons followed by violent volume explosion. Either phothermal or photochemical driven processes can generate significant mechanical stresses in the medium. The PFA is generally limited to intensities below $10^4$ W/cm$^2$.

If air is the transport medium, PFA often dominates during ablation with CW lasers and chopped-wave beams of relatively long light exposures (>ms), or long duration pulse systems. An important advantage of operation in this regime is that energy coupling is dominated by WL-dependent material absorption (of intact and decomposed components of the tissue) throughout the pulse duration. Enhanced ablation may thus be affected by manipulation of the optical penetration depth. Ablation characteristics also can be effectively controlled by manipulation of the optical penetration depth with respect to exposure times and the tissues thermal and mechanical characteristics. Unfortunately, treatment results obtained in this regime of operation are often not satisfactory due to excessive thermal damage to bordering regions. Also, attempts to enhance ablation in this region by increasing laser power are always accompanied by increased photothermal and photomechanical effects, thus further compromising adjacent tissue safety.

When expulsion of material takes place, some of the ejected material can be ionized and through the process of inverse bremsstrahlung, the material is further broken down by the optical field to produce an optically thick plasma. Once plasma formation threshold is exceeded, plasma-mediated interactions dominate the ablation process and will, in turn, significantly alter the entire interaction process. The generation of plasma can disrupt the coupling of laser light from the tissue or it may enhance the coupling process. In the normal pulse laser regimes of the lasers examined in this study, plasma is always observed when an efficient ablation is observed. Plasma is also always present in the nanosecond pulse ablation regimes that we tested here and in our other nanosecond pulse laser studies on dentin. In the nanosecond regime, however, AR are consistently poor—on the order of 1–3 μm/pulse.

When air is the transport medium and laser intensities are greater than the plasma formation threshold, laser-supported combustion (LSC) waves can be ignited. These waves occur at intensities ranging from ~ $10^4$–$10^7$ W/cm$^2$ (in both pulsed and CW systems). LSC waves are ignited in the ejected vapor. LSC waves propagate away

from the target surface along the incoming beam path, in the process driving a shock wave in the air just ahead of them.

The exact characteristics of light coupling to the material when plasma is formed depends on the laser parameters (energy, spot size, and pulse duration) as well as on transport medium pressure and the target material. The low density of the LSC waves allows laser light to reach and heat the plasma adjacent to the surface and plasma temperatures can often exceed 20,000°K. The hot plasma (which is localized and close to the surface) radiates again in the UV. This secondary radiation is strongly absorbed by most surfaces. Energy coupling to the optically irradiated zone is enhanced because the secondary radiation is efficiently transferred from the hot, high pressure plasma to the target surface. As long as the LSC wave expansion remains nearly one-dimensional, the plasma-radiated light remains localized in the original optical zone and local coupling is enhanced.

In this power density regime, once plasma is formed, coupling of subsequent photons to the surface is dominated by the plasma and is relatively insensitive to the laser WL. Lasers with PD ranging from microseconds to a few hundred microseconds often fall into this category as are the two normal pulse lasers in our experiments. In particular, if we consider the normal pulse lasers tested by us [see also 17], we note that AR are essentially of the same order of magnitude in all of these systems (e.g., 10–20 μm/p for pulse energies of 80 mJ, with the exception of the Er:YSGG where AR at one Hz are one and a half to two times larger). This is particularly intriguing in view of the fact that these WL absorption characteristics span four orders of magnitude. Again, these considerations, together with our observation that significant AR are accompanied by laser-induced sparks, strongly suggest that plasma may be a common, unifying mechanism in the AR behavior of all these very different systems.

Plasmas initiation does not always take place in such systems where deeper penetration and surface characteristics prevent initial ionization. In such cases, "initiators," a layer of highly absorbing matter, has often been used to ensure high heat deposition on the surface and subsequent ionization. Indeed, initiator use yields remarkably uniform, high AR, which are similar to those observed with our normal mode systems.

At high intensities ($> 10^7$ W/cm$^2$), a laser-supported detonation (LSD) wave is ignited. A hot high-pressure front is formed behind the LSD wave and serves as an absorption barrier to incoming laser light. This absorption zone propagates away from the surface and reradiates energy as UV light over a larger target area, thus reducing local energy deposition. The nanosecond Nd:YAG as well as those of other nanosecond systems we investigated in the past (ArF, XeCl) fall into this high intensity category. Here, too, all systems show remarkably similar behavior in spite of large tissue-absorption variations, and in spite of the possibility of direct, efficient coupling of UV light due to their bond-breaking high energy photons. Again, it is suggested that these similarities are a consequence of the unifying, high intensity laser-induced plasma regime of operation, which, once initiated, dominates the interaction.

Temperature characteristics (within the limitation of the relatively slow frame acquisition time of the thermal camera) also show identifying characteristics of the two plasma regimes. They show the temperatures of the nanosecond pulse lasers to be considerably lower than those of the normal pulse lasers for the corresponding pulse energies and PRR. Acquisition times, however, are too long to monitor temperature distributions on the time scale of the PD and are, therefore, unable to distinguish between heat distributions in the plasma, the exposed surface, or the plume of ejected debris. Faster times as well as spatial discrimination should enable us to resolve the contributing source in the future. Due to its slow acquisition time (30 ms/frame), the thermal camera measurements correspond primarily to lingering surface effects. They show that surface temperatures are greatest with the Er:YSGG intermediate with the Ho:YSGG and smallest with the ns Nd:YAG. Again, nanosecond Nd:YAG temperatures are very similar to those observed with the nanosecond Excimer lasers, whereas those of the Er:YSGG and Ho:YSGG are of the same order of magnitude as the temperatures of the normal pulse Nd:YAG.

It is also interesting to compare the dependence of surface temperatures and AR on PRR in the nanosecond Nd:YAG and normal pulse Ho:YSGG. Whereas increased PRR clearly corresponds to a direct increase in surface temperatures as heat is retained in the tissue between subsequent pulses, the AR per pulse does not seem to be strongly affected by this parameter. This pattern was also observed in our earlier studies on excimer lasers.

The fact that AR are generally not very sensitive to PRR implies that the pulse-to-pulse re-

sidual heating does not play a very important role in the ablation process. If ablation with the three IR lasers investigated here was primarily defined by thermal mechanisms, a greater role of PRR should be expected since the thermal camera data show a very significant surface temperature dependence on PRR. The fact that this is not the case may support our hypothesis that plasma-mediated mechanisms are dominating the interactions. Plasma formation and its subsequent heating requires rapid temperature rise associated with the ultrafast heating of the very short PD lasers. These intensities and the subsequent temperature increases are defined by the laser pulse energy, PD, and spot size but are *not* very sensitive to the pulse-to-pulse residual heating. Thus the principle parameters determining AR are the laser PD and pulse energy, which are also critical in determining plasma regime characteristics. The only exception to this very weak dependence of AR on PRR is the Er:YSGG data. Here, AR at the higher PRR are difficult to interpret and are a subject of further investigation.

## ACKNOWLEDGMENTS

We thank Lih-Huei L. Liaw, Peter Ho, Jack Fujishige, Eric Cheung, and Vivian Sung for their valuable help. We also thank Elizabeth Berry for her expert help with the manuscript. This work was supported by NIH grant 5P41RR01192, by Department of the Navy grant N00014-90-0-0029, and by Department of Energy grant DE-FG0391ER61227.

## REFERENCES

1. Willenborg GC. Dental laser applications: emerging to maturity. Lasers Surg Med 1989; 9:309–313.
2. Stabholz A, Khayat A, Ravanshad S, McCarthy D, Neev J, Torabinejad M. Effects of Nd:YAG laser on apical seal of teeth after apicoectomy and retrofill. J Endodontics 1992; 18:371–375.
3. Stabholz A, Khayat A, Weeks D, Neev J, Torabinejad M. Scanning electron microscopic study of the apical dentin surfaces lased with Nd:YAG laser following apicetomy and retrofill. International Endodontics J 1992; 25:288–291.
4. White JM, Goodis HE, Kudler JJ, Eakle WS, Neev J. Histologic and SEM evaluation of caries removal and restoration in enamel and dentin using a pulsed fiber optic delivered Nd:YAG laser. In Laser Society: Advanced Characterization, Therapeutics, and Systems IV. Anderson RR, Ed Proc. The International Society for Optical Engineering, 1994; 2128:439–52.
5. Neev J, Goodis HE, White JM. Thermal characteristics during Nd:YAG and carbon dioxide laser application on enamel and dentin. In Laser Surgery: Advanced Characterization, Therapeutics, and Systems, IV. Anderson RR, Ed Proc. The International Society for Optical Engineering 1994; 2128:424–430.
6. White JM, Goodis HE, Setcos JC, Eakle WS, Hulscher BE, Rose CL. Effects of pulsed Nd:YAG laser energy on human teeth: A three year follow-up study. JADA 1993; 124:45–51.
7. Goodis HE, White JM, Harlan L. Absence of pulpal response from Nd:YAG laser exposure on enamel. J Dent Res 1991; 71:162 Abs 449.
8. White JM, Goodis HE. Rat pulp response to Nd:YAG laser exposure to dentin. J Dent Res 1993; 72:124, Abs 168.
9. White JM, Goodis HE, Tran KT, Ho W, Kudler JJ. In vivo pulpal response to Nd:YAG laser on dentin. J Dent Res 1994; 73:318, Abs 1732.
10. White JM, Goodis HE, Sekandari N, Fraser D, Rahman A. Caries removal and restoration using a Nd:YAG laser. J Dent Res 1994; 73:410, Abs 2465.
11. White JM, Goodis HE, Hennings D, Ho W, Hipona CT. Dentin ablation rate using Nd:YAG and Er:YAG lasers. J Dent Res 1994; 73:318, Abstract 1733.
12. Hibst R, Keller U. Experimental studies of the application of the Er:YAG laser on dental hard substances: I. Measurement of the ablation rate. Lasers Surg Med 1989; 9:352–357.
13. Keller U, Hibst R. Experimental studies of the application of the Er:YAG laser on dental hard substances: II. Light microscopy and SEM investigations. Lasers Surg Med 1989; 9:345–351.
14. Paghdiwala AF. Root resection of endodontically treated teeth by Er:YAG laser radiation. Proc SPIE 1991; 24: 150–159.
15. Neev J, Liaw LL, Raney DV, Fujishige JT, Ho PT, Berns MW. Selectivity and efficiency in the ablation of hard dental tissue with ArF pulsed excimer lasers. Lasers Surg Med 1991; 11:499–510.
16. Neev J, Stabholz A, Liaw LL, Torabinejad M, Fujishige JT, Ho PH, Berns MW. Scanning electron microscopy and thermal characteristics of dentin ablated by a short-pulse XeCl laser. Lasers Surg Med 1993; 13: 3:353–361.
17. White JM, Goodis HE, Hennings D, Ho W, Hipona CT. Dentin ablation rate using Nd:YAG and Er:YAG lasers. J Dent Res 1994; 73:318, Abs 1733.
18. White JM, Marshall SJ, Marshall GW, Strawn SE, Goodis HE, Law JG. Spectrophotometric analysis of dentin as a function of intra-tooth location. J Dent Res 1994; 73: 214, Abs 903.
19. White JM, Goodis HE, Marshall JS, Marshall GW. Sterilization of teeth by gamma radiation. J Dent Res 1994; 73(9):1560–1567.
20. Neev J, Raney DV, Whalen WE, Fujishige JT, Ho PD, McGrann JV, Berns MW. Dentin ablation with two excimer lasers: A comparative study of physical characteristics. Lasers Life Sci 1992, 4(3):1–25.
21. Koren G, Yeh JTC. Emission spectra and etching of polymers and graphite irradiated by excimer lasers. J Appl Physics 1984; 56(7):2120–2126. Abs.
22. Jacques SL. Role of tissue optics and pulse duration of tissue effects during high-power laser irradiation. Applied Optics, 1993; 32(13):2447–2454.
23. Walsh JT, Deutsch TF. Er:YAG laser ablation of tissue: Measurement of ablation rates. Lasers Surg Med 1989; 9(4):327.